

1 **Brief Communication**

2 **Co-seismic displacement on October 26 and 30, 2016 ( $M_w$  5.9 and 6.5) -**  
3 **earthquakes in central Italy from the analysis of a local GNSS network**

4  
5 De Guidi Giorgio<sup>1,2</sup>, Vecchio Alessia<sup>1</sup>, Brighenti Fabio<sup>1</sup>, Caputo Riccardo<sup>3,4,5</sup>, Carnemolla Francesco<sup>1</sup>, Di Pietro  
6 Adriano<sup>1</sup>, Lupo Marco<sup>1</sup>, Maggini Massimiliano<sup>3,5</sup>, Marchese Salvatore<sup>1</sup>, Messina Danilo<sup>1</sup>, Monaco  
7 Carmelo<sup>1,2</sup>, Naso Salvatore<sup>1</sup>

9 1) Department of Biological, Geological and Environmental Sciences, University of Catania, Italy

10 2) CRUST, UR-UniCT, Catania, Italy

11 3) Department of Physics and Earth Sciences, University of Ferrara, Italy

12 4) Research and Teaching Center for Earthquake Geology, Tyrnavos, Greece

13 5) CRUST, UR-UniFE, Ferrara, Italy

14 *Corresponding author: G. De Guidi (deguidi@unict.it)*

16 **1 - Abstract**

17 On August 24<sup>th</sup> 2016 a strong earthquake ( $M_w = 6.0$ ) affected Central Italy and an intense seismic sequence  
18 started. Field observations, DInSAR analyses, preliminary focal mechanisms as well as the distribution of  
19 aftershocks suggested the reactivation of the northern sector of the Laga Fault, whose southern part was  
20 already rebooted during the 2009 L'Aquila sequence, and of the southern segment of the Monte Vettore  
21 Fault System (MVFS). Based on these preliminary information and following the stress-triggering concept  
22 (Stein et al., 1999; Steacy et al., 2005), we tentatively identified a potential fault zone most vulnerable to  
23 future seismic events just north of the earlier epicentral area. Accordingly, we planned a local geodetic  
24 network consisting of five new GNSS (Global Navigation Satellite System) stations located at few km of  
25 distance on both sides of the MVFS. This network was devoted to picture out, at least partially but in some  
26 detail, the possible northward propagation of the crustal network ruptures. The building of the stations and  
27 a first set of measurements were carried out during a first campaign (September 30<sup>th</sup> October 2<sup>nd</sup>, 2016). On  
28 October 26<sup>th</sup> 2016, immediately north of the epicentral area of the August 24<sup>th</sup> event, another earthquake  
29 ( $M_w = 5.9$ ) indeed occurred, followed four days later (October 30<sup>th</sup>) by the mainshock ( $M_w = 6.5$ ) of the whole  
30 2016 Summer-Autumn seismic sequence. Our local geodetic network was fully affected by the new events  
31 and therefore we performed a second campaign soon after (November 11<sup>th</sup>-13<sup>th</sup>, 2016). In this brief note, we  
32 provide the results of our geodetic measurements that registered the co-seismic and immediately post-  
33 seismic deformation of the two major October shocks documenting in some details the surface deformation  
34 close to the fault trace. We also compare our results with the available surface deformation field of the  
35 broader area, obtained on the basis of the DInSAR technique, and show an overall good fit.

37 **2 - Geological framework**

38 The central Apennines are characterized by northeast-verging thrust-propagation folds, involving Mesozoic-  
39 Tertiary sedimentary successions. During the 2016 sequence, coseismic deformation was recorded at the  
40 rear of the Sibillini Thrust that separates the homonymous mountain chain from the Marche-Abruzzi foothills  
41 (Fig. 1). According to many studies in the area, the main thrust-related anticlines and associated reverse faults  
42 have been dissected and/or inverted by NNW-SSE trending Quaternary normal and oblique-slip faults (Figs.

43 1 and 2), in particular by the Norcia Fault System (NFS) (Calamita and Pizzi, 1992; Calamita et al., 1982; 1995;  
44 1999; 2000; Blumetti et al., 1990; Blumetti, 1995; Brozzetti and Lavecchia, 1994; Cello et al., 1998; Galadini  
45 and Galli, 2000; Pizzi and Scisciani, 2000; Pizzi et al., 2002; Boncio et al., 2004 Galadini, 2006; Gori et al., 2007)  
46 and the Mt. Vettore Fault System (MVFS) (Calamita and Pizzi, 1991; Coltorti and Farabollini, 1995; Cello et  
47 al., 1997; Pizzi et al., 2002; Galadini and Galli, 2003; Pizzi and Galadini, 2009) (Figs. 1 and 2). Conversely,  
48 Pierantoni et al. (2013) suggest that the major Mt. Sibillini Thrust has not been yet dissected by quaternary  
49 normal faulting, though some fresh morphological scarps with free faces in the carbonate bedrock and/or  
50 affecting recent slope deposits have been observed and attributed to the local seismic activity.

51 Within a distance of few tens of kilometers, large evidence of ground deformation has been provided by  
52 several recent earthquakes, like the 1979 Norcia event ( $M_w$  5.9, reactivating the Norcia Fault; e.g. Deschamps  
53 et al., 2000), the 1984 Gubbio ( $M_w$  5.6, Gubbio Fault; e.g. Boncio et al., 2004), the 1997 Colfiorito ones ( $M_w$   
54 5.7, 6.0 and 5.6, Calforito-Cesi-Costa fault system; e.g. Cello et al., 1997), the 2009 L'Aquila mainshock and  
55 the Campotosto aftershock ( $M_w$  6.3 and 5.4, Upper Aterno Valley-Paganica fault system and Gorzano Fault;  
56 Blumetti et al. 2013) and basically the same occurred with the 2016 seismic sequence.

57 Surface evidence of the August 24<sup>th</sup> (e.g., EMERGEO WG, 2016; Livio et al., 2016; Aringoli et al., 2016) was  
58 mainly observed in the area of the Laga basin (Gorzano Fault), which corresponds to the footwall block of  
59 Sibillini Thrust, while debated ground ruptures (e.g. Valensise et al., 2016) also occurred in the southern  
60 sector of the MVFS, which belongs to the hanging-wall block of the orogenic structure. In contrast, as a  
61 consequence of the mainshock of October 30<sup>th</sup>, the entire western flank of the Monte Vettore was affected  
62 by impressive geological effects and clear coseismic ruptures mapped for a minimum length of 15 km,  
63 between the Castelluccio di Norcia and Ussita (EMERGEO WG, 2016) (Fig. 2). The surface ruptures occurred  
64 along distinct fault splays of the fracture system. For example, along the western slope of Monte Vettore  
65 three main west dipping splays were activated together with two antithetic branches (Figs. 1 and 2). The  
66 observed vertical offset reached 2 m along the main west dipping fault segment, where the slickensides show  
67 a prevalent dip-slip component of motion. Vertical displacements of a few centimetres were also recorded  
68 along an antithetic surface rupture bordering to the west the Castelluccio plain, about 6-7 km far from the  
69 main ground rupture, possibly connected to a secondary fault (Figs. 1B and 2).

70 It is worth to note that the August-October earthquakes occurred in a sector of the Central Apennines  
71 characterized by high geodetic strain-rates (e.g., Devoti et al., 2011; D'Agostino 2014), where several  
72 continuous GNSS stations are operating.

73

### 74 **Implementation and Analysis of UNICT discrete GPS stations**

75 Following the August 24<sup>th</sup>,  $M_w$  6.0 earthquake, the GEOMATIC Working Group of the Catania University  
76 (UNICT) in collaboration with the SpinOff EcoStat s.r.l. and researches of the Ferrara University, started a  
77 detailed monitoring of ground deformation in the epicentral area using the Global Navigation Satellite System  
78 (GNSS) technique. The GNSS measurement has been made in static mode, setting the time at 6 hours and  
79 post-processing position, in order to reduce tropospheric error and using IGS precise products for orbits. The  
80 IGS station coordinates were kept fixed in order to align the final velocity field with the WGS84 reference  
81 frame. The measurement mode, adopted for receiver-satellite range determination, is performed with a  
82 double frequency receiver, allowing phase and code measurements on the signal carrier (L1, L2, C1, P1, P2,  
83 S1, S2). The coordinates estimation is based on the principle of minimum squares.

84 For this aim, five GNSS stations have been installed on new benchmarks purposely built by the working group  
85 and here referred to as UNICT network (Fig. 3). These new stations have been realized taking into account  
86 the following criteria:

- 87 I. the distribution of the existing permanent and discrete measurement benchmarks belonging to  
88 different networks that were active before the event of 24 August (IGM; RING; CAGEONET; DPC;  
89 ISPRA) (Fig. 2B).  
90 II. the seismotectonic setting of the area in relation to the macroseismic data and to the reactivated  
91 structures (Figs. 1 and 2);  
92 III. surface and deep geometry of the major faults related to tectonic setting (Fig. 1B).  
93 IV. the lack of possible gravitational instabilities in both static and dynamic conditions in sites where the  
94 new benchmarks are built.

95 Based on the above criteria, the working group installed the benchmarks at the bottom of both western and  
96 eastern slopes of Mt. Vettore, within an area about 8 km-long and 5 km-wide in the N-S and E-W directions,  
97 respectively. The distribution of the benchmarks was planned for reconstructing the principal deformation  
98 zone developed as a consequence of the August 24<sup>th</sup> event (Fig. 2) and particularly with points:

- 99 I. much closer to the epicentral area than the already existing ones belonging to other networks (Fig.  
100 2B);  
101 II. characterized by equivalent distances from the reactivated Mt. Vettore Fault segments (Fig. 2);  
102 III. within a distance of 30 km from the closest permanent network points that have been not affected  
103 by deformation, therefore allowing a rigorous elaboration during the post processing phases.

104 The building of GNSS monument on the UNICT benchmarks consists of the following steps (Fig. 3):

- 105 I. selection of a suitable site, corresponding to a massive rocky outcrop or a man-made monument with  
106 foundation; these sites must be also free of structures or other natural elements in the surroundings  
107 that may constitute a perturbation during recording;  
108 II. testing of GPS signal reception by short-term exams, and control of parameters set through the  
109 quality check carried out by software TEQC ([http://www.unavco.org/software/data-  
110 processing/teqc/teqc.html](http://www.unavco.org/software/data-processing/teqc/teqc.html));  
111 III. implementation of the hole for housing the bushing and check of its verticality; the hole has a  
112 diameter of 35 mm and a depth of 100 mm, it is realized through small-sized battery-powered  
113 equipment (Makita DHR243 hammer drill);  
114 IV. fixing and anchoring of the knurled steel bushing (length 67 mm and diameter 20 mm), with bi-  
115 component resins or quick-setting cements;  
116 V. following the cementation to the artefact or to rocky outcrop, a male-male threaded bar can be  
117 screwed in until end of stroke; the height could be variable and this fact is considered in the data  
118 processing. We have used a threaded bar 670 mm-high.

119 The GPS monument is thus completed with a GNSS receiver TOPCON, mounting a HiPer V antenna,  
120 characterized by 226 channels and position accuracy with band L1+L2 in Static mode of 3 mm + 0.1 ppm  
121 (horizontal) and 3.5 mm + 0.4 ppm (vertical). All registrations last six hours in static mode.

122 Following the August 24<sup>th</sup> event, at the end of September 2016 the working group carried out the first survey  
123 campaign with the installation of five UNICT benchmarks: two stations were located east of the Mt. Vettore  
124 fault (VTE1,VTE2), the other three (VTW3,VTW4, VTW5) west of the fault (Figs. 4 and 5). During November  
125 2016 (*i.e.* after the October 30<sup>th</sup> event), a second field campaign was carried out following the same  
126 procedure and using the same instrumentation. The second set of measurements allowed us to record the  
127 co-seismic displacement caused by both the  $M_w$  5.9 and  $M_w$  6.5 events of October 26<sup>th</sup> and 30<sup>th</sup>, respectively  
128 (doy (day of year) 2016/274 and doy 2016/318).

129 The data from survey-mode GNSS stations have been downloaded and processed using TOPCON Magnet  
130 analysis software evaluating co-seismic solutions and comparing with AUSPOS web-based online services for  
131 GPS data processing (Ocalan et al., 2013), whose engine is based on Bernese 5.2 software. In the software  
132 TOPCON, the baseline is automatically created for any pair of static occupations, where we set up six hours  
133 for Minimum Duration and the baselines max length of 50 km, cut-off angle of 15°, troposphere model Goad-  
134 Goodman and, finally, meteo model NRLMSISE (neutral temperature and densities in Earth's atmosphere).  
135 For the analyses we referred to the measurement of a stable reference frame of five GNSS stations belonging  
136 to the RING (Rete Integrata Nazionale GPS) network, with a maximum baseline length of 50 km, using stations  
137 CESI, GNAL, GUMA, MTER and MTTO (Figs. 4 and 5). Data processing has been carried out with adjustment  
138 by Least Squares and a TAU Criterion.

139

#### 140 **Concluding remarks**

141 Using the GNSS technique, we investigated the ground deformation occurred in the surroundings of the Mt.  
142 Vettore Fault System during the 2016 central Italy seismic sequence. This foresight action allowed us to  
143 record the co-seismic and part of the post-seismic deformation of the second and third (strongest) events  
144 ( $M_w$  5.9 and  $M_w$  6.5) on October 26<sup>th</sup> and October 30<sup>th</sup>, 2016, respectively. Taking into account the geometry  
145 of the fault system in the broader epicentral area and following the stress-triggering concept (Stein et al.,  
146 1999; Steacy et al., 2005), we have identified a potential fault zone most vulnerable to future seismic events  
147 just north of the fault segment reactivated during the August 24<sup>th</sup> earthquake (Figs. 2B and 5). With this in  
148 mind, in order to measure the post seismic deformation and to possibly record the potential migration of the  
149 co-seismic process, we selected some sites and built five new GNSS benchmarks, distributed east and west  
150 of the northern-central segment of the Mt. Vettore Fault System. For site selection we also considered the  
151 presence and distribution of other benchmarks located before the second seismic event by other research  
152 groups (IGM; RING; CAGEONET; DPC; ISPRA). The epicentral location of the October events confirmed our  
153 guess and then we performed soon after a second campaign of measurements for quantifying the relative  
154 motion of the stations.

155 The measured deformation (with 95% confidence errors) is characterised by both horizontal and vertical  
156 movements. In particular, the east benchmark VTE1 recorded 312 mm of eastward horizontal displacement  
157 and 29 mm of upward motion, while the VTE2 recorded 282 mm of eastward horizontal displacement and  
158 67 mm of upward component of motion. On the contrary, all three western benchmarks recorded westward  
159 horizontal displacements (419, 288 and 26 mm) and subsidence (707, 288 and 769 mm) for stations VTW5,  
160 VTW4 and VTW3, respectively. In conclusion, we documented ca. 730 mm of ENE-WSW lengthening on a  
161 distance of 7 km in correspondence of the northern sector of the Mt. Vettore Fault Segment, while the off-  
162 fault vertical displacement between footwall and hanging-wall blocks was 736 mm.

163 We also compared our results with the displacement distribution obtained by other research group with  
164 DInSAR techniques, recorded between October 26<sup>th</sup> 2016 (pre-event images) and November 1<sup>st</sup> 2016 (post-  
165 event images), and other GNSS stations, active before the second seismic event. In Fig. 5 we may observe the  
166 overall consistency of the different approaches and datasets.

167

168

169 **Acknowledgments** This paper was carried out with the financial support of the University of Catania (FIR  
170 2014 Project Code 2C7D79, Scientific Supervisor: G. De Guidi) and University Spin Off of Catania EcoStat s.r.l.

171

172

#### 173 **References**

174 Anzidei M., Baldi P. and Serpelloni E. (2008). The coseismic ground deformations of the 1997 Umbria-Marche  
175 earthquakes: A lesson for the development of new GPS networks, *Ann. Geophys.*, 51(2–3), 27– 43.

176 Anzidei M. and Pondrelli S. (Eds) (2016). The Amatrice seismic sequence: preliminary data and results, *Annals*  
177 *of Geophysics*, 59, Fast Track 5, 2016

178 Aringoli D., Farabollini P., Giacometti M., Materazzi M., Paggi S., Pambianchi G., Pierantoni P.P., Pistolesi E.,  
179 Pitts A. and Tondi E. (2016). The August 24th 2016 Accumoli earthquake: surface faulting and Deep-  
180 Seated Gravitational Slope Deformation (DSGSD) in the Monte Vettore area. *Ann. Geophysics*, 59, fast  
181 track 5, 2016; doi: 10.4401/ag-7199.

182 Blumetti A.M. (1995). Neotectonic investigations and evidence of paleoseismicity in the epicentral area of  
183 the January-February 1703, Central Italy, earthquakes. In: Serva, L. & Slemmons, D. B., (eds.):  
184 *Perspectives in paleoseismology*. Association of Engineering Geologists, spec. publ. 6, 83-100.

185 Blumetti A.M., Dramis F., Gentili B. and Pambianchi G. (1990). La struttura di M. Alvagnano-Castel Santa  
186 Maria nell'area nursina: aspetti geomorfologici e sismicità storica. *Rend. Soc. Geol. It.*, 13, 71-76.

187 Blumetti A.M., Guerrieri L. and Vittori E. (2013). The primary role of the Paganica-San Demetrio fault system  
188 in the seismic landscape of the Middle Aterno Valley basin (Central Apennines). *Quaternary*  
189 *International*, 288, 183-194, doi: 10.1016/j.quaint.2012.04.040.

190 Boncio P., Lavecchia G., and Pace B (2004). Defining a model of 3D seismogenic sources for Seismic Hazard  
191 Assessment applications: The case of central Apennines (Italy). *Journal of Seismology* 8: 407–425.

192 Brozzetti F. and Lavecchia G. (1994). Seismicity and related extensional stress field; the case of the Norcia  
193 seismic zone (central Italy). *Annales Tectonicae* 8, 36–57

194 Calamita F. and Pizzi A., 1992. Tettonica quaternaria nella dorsale appenninica umbro-marchigiana e bacini  
195 intrappenninici associati. *Studi Geologici Camerti*, spec. vol. 1992/1, 17-25.

196 Calamita F., Coltorti M., Deiana G., Dramis F. and Pambianchi G. (1982). Neotectonic evolution and  
197 geomorphology of the Cascia and Norcia depression (Umbria-Marche Apennine). *Geografia Fisica e*  
198 *Dinamica Quaternaria*, 5, 263-276.

199 Calamita F., Pizzi A., Romano A., Roscioni M., Scisciani V. and Vecchioni G. (1995). La tettonica quaternaria  
200 nella dorsale appenninica umbro-marchigiana: una deformazione progressiva non coassiale. *Studi Geol.*  
201 *Camerti*, vol. spec.1995/1, 203-223.

202 Calamita F., Coltorti M., Pieruccini P. and Pizzi A. (1999). Evoluzione strutturale e morfogenesi plio-  
203 quaternaria dell'appennino umbro-marchigiano tra il preappennino umbro e la costa adriatica. *Bollettino*  
204 *della Società Geologica Italiana*, 118, 125-139.

205 Calamita F., Coltorti M., Piccinini D., Pierantoni P.P., Pizzi A., Ripepe M., Scisciani V. and Turco E. (2000).  
206 Quaternary faults and seismicity in the Umbro-Marchean Apennines (central Italy). *Journal of*  
207 *Geodynamics* 29, 245–264.

208 Cello G., Mazzoli S., Tondi E. and Turco E. (1997). Active tectonics in the Central Apennines and possible  
209 implications for seismic hazard analysis in peninsular Italy. *Tectonophysics*, 272, 43-68.

210 Cello G., Deiana G., Mangano P., Mazzoli S., Tondi E., Ferrelì L., Maschio L., Michetti A.M., Serva L. and Vittori  
211 E. (1998). Evidence for surface faulting during the September 26, 1997, Colfiorito (Central Italy)  
212 earthquakes. *Journal of Earthquake Engineering*, 2, 1-22.

213 Coltorti M. and Farabollini P. (1995). Quaternary evolution of the Castelluccio di Norcia Basin. *Il Quaternario*,  
214 8, 149-166.

215 Deschamps A., Courboux F., Gaffet S., Lomax A., Virieux J., Amato A., Azzara A., Castello B., Chiarabba C.,  
216 Cimini G.B., Cocco M., Di Bona M., Margheriti L., Mele F., Selvaggi G., Chiaraluce L., Piccinini D. and  
217 Ripepe M. (2000). Spatio-temporal distribution of seismic activity during the Umbria-Marche crisis, 1997.  
218 *Journal of Seismology* 4: 377–386.

219 Devoti R., Esposito A., Pietrantonio G., Pisani A.R. and Riguzzi F. (2011). Evidence of large scale deformation  
220 patterns from GPS data in the Italian subduction boundary. *Earth and Planetary Science Letters*, 311,  
221 230–241, doi:10.1016/j.epsl.2011.09.034.

222 EMERGEO W.G. (2016). Coseismic effects of the 2016 Amatrice seismic sequence: first geological results.  
223 *Ann. Geophysics*, 59, fast track 5, 2016; doi: 10.4401/ag-7195

224 Galadini F. and Galli P. (2000). Active tectonics in the Central Apennines (Italy) - Input data for seismic hazard  
225 Assessment. *Natural Hazards*, 22, 225-270.

226 Galadini F. and Galli P. (2003). Paleoseismology of silent faults in the central Apennines (Italy): the Mt. Vettore  
227 and Laga Mts. faults. *Annali di Geofisica*, 46, 815-836.

228 Galvani A., Anzidei M., Devoti R., Esposito A., Pietrantonio G., Pisani A., Riguzzi F. and Serpelloni E. (2012).  
229 The interseismic velocity field of the central Apennines from a dense GPS network. *Ann. Geophys.* 55, 5,  
230 2012; doi: 10.4401/ag-5634.

231 Gori S., Dramis F., Galadini F. and Messina P. (2007). The use of geomorphological markers in the footwall of  
232 active faults for kinematic evaluations: examples from the central Apennines. *Bollettino della Società*  
233 *Geologica Italiana*, 126, 365-374.

234 GdL-INGV (Gruppo di Lavoro INGV sul terremoto in centro Italia) (2016). Summary report on the October 30,  
235 2016 earthquake in central Italy Mw 6.5, doi: 10.5281/zenodo.166238

236 Harris R.A. (1998). Introduction to special section: Stress triggers, stress shadows, and implications for seismic  
237 hazard. *J. Geophys. Res.* 103, 347–358.

238 Kilb D., Gomberg J. and Bodin P. (2000). Triggering of earthquake aftershocks by dynamic stresses. *Nature*  
239 408, 570–574.

240 Livio F., Michetti A.M., Vittori E., Gregory L., Wedmore L., Piccardi L., Tondi E., Roberts G. and Central Italy  
241 Earthquake Working Group (2016): Surface faulting during the August 24, 2016, Central Italy  
242 earthquake (Mw 6.0): preliminary results. *Ann. Geophysics*, 59, fast track 5, 2016; doi: 10.4401/ag-7197

243 Pierantoni P., Deiana G. and Galdenzi S. (2013). Stratigraphic and structural features of the Sibillini mountain  
244 (Umbria-Marche- Apennines, Italy). *Ital. J. Geosci. (Boll. Soc. Geol. It.)* Vol.132 No.3, pp. 497-520.

245 Mantovani E., Viti M., Babbucci D., Cenni N., Tamburelli C., Vannucchi A., Falciani F., Fianchisti G., Baglione  
246 M., D’Intinosante V. and Fabbroni P. (2011). Sismotettonica dell’Appennino Settentrionale. Implicazioni  
247 per la pericolosità sismica della Toscana. Regione Toscana, Centro stampa Giunta Regione Toscana,  
248 Firenze, pagg. 88 (<http://www.rete.toscana.it/sett/pta/sismica/index.shtml>).

249 Pizzi A. and Galadini F. (2009). Pre-existing cross-structures and active fault segmentation in the northern-  
250 central Apennines (Italy), *Tectonophysics*, 476(1-2), 304–319, doi:10.1016/j.tecto.2009.03.018.

251 Pizzi A. and Scisciani V. (2000). Methods for determining the Pleistocene–Holocene component of  
252 displacement on active faults reactivating pre-Quaternary structures: examples from the central  
253 Apennines (Italy). *Journal of Geodynamics* 29, 445–457.

254 Pizzi A., Calamita F., Coltorti M. and Pieruccini P. (2002). Quaternary normal faults, intramontane basins and  
255 seismicity in the Umbria-Marche- Abruzzi Apennine ridge (Italy): contribution of neotectonic analysis to  
256 seismic hazard assessment. *Boll. Soc. Geol. It., Spec. Publ.*, 1, 923–929.

257 Pizzi A., Calamita F., Coltorti M. and Pieruccini P. (2002). Quaternary normal faults, intramontane basins and  
258 seismicity in the Umbria-Marche- Abruzzi Apennine ridge (Italy): contribution of neotectonic analysis to  
259 seismic hazard assessment. *Boll. Soc. Geol. It., Spec. Publ.*, 1, 923–929.

260 Pizzi A. and Galadini F. (2009) Pre-existing cross-structures and active fault segmentation in the northern-  
261 central Apennines (Italy). *Tectonophysics*. 476, 304-319.

262 Steacy S., Gomberg J. and Cocco M. (2005). Introduction to special section: Stress transfer, earthquake  
263 triggering, and time-dependent seismic hazard. *J. Geophys. Res.* 110, B05S01.

264 Stein R.S. (1999). The role of stress transfer in earthquake occurrence. *Nature* 402, 605–609.

265 Valensise G., Vannoli P., Basili R., Bonini L., Burrato P., Carafa M.C., Fracassi U., Kastelic V., Maesano F.E.,  
266 Tiberti M. and Tarabusi G. (2016). Fossil landscapes and youthful seismogenic sources in the central  
267 Apennines: excerpts from the 24 August 2016, Amatrice earthquake and seismic hazard implications.  
268 Ann. Geophysics, 59, fast track 5, 2016; doi: 10.4401/ag-7215.

269

270 **Website links**

271 <http://iside.rm.ingv.it>

272 <http://ring.gm.ingv.it>

273 <http://www.igmi.org/geodetica/>

274 [http://www.irea.cnr.it/index.php?option=com\\_k2&view=item&id=761:nuovi-risultati-sul-terremoto-del-  
275 30-ottobre-2016-ottenuti-dai-radar-dei-satelliti-sentinel-1](http://www.irea.cnr.it/index.php?option=com_k2&view=item&id=761:nuovi-risultati-sul-terremoto-del-30-ottobre-2016-ottenuti-dai-radar-dei-satelliti-sentinel-1)

276 [http://www.irea.cnr.it/index.php?option=com\\_k2&view=item&id=761:nuovi-risultati-sul-terremoto-del-  
277 30-ottobre-2016-ottenuti-dai-radar-dei-satelliti-sentinel-1](http://www.irea.cnr.it/index.php?option=com_k2&view=item&id=761:nuovi-risultati-sul-terremoto-del-30-ottobre-2016-ottenuti-dai-radar-dei-satelliti-sentinel-1)

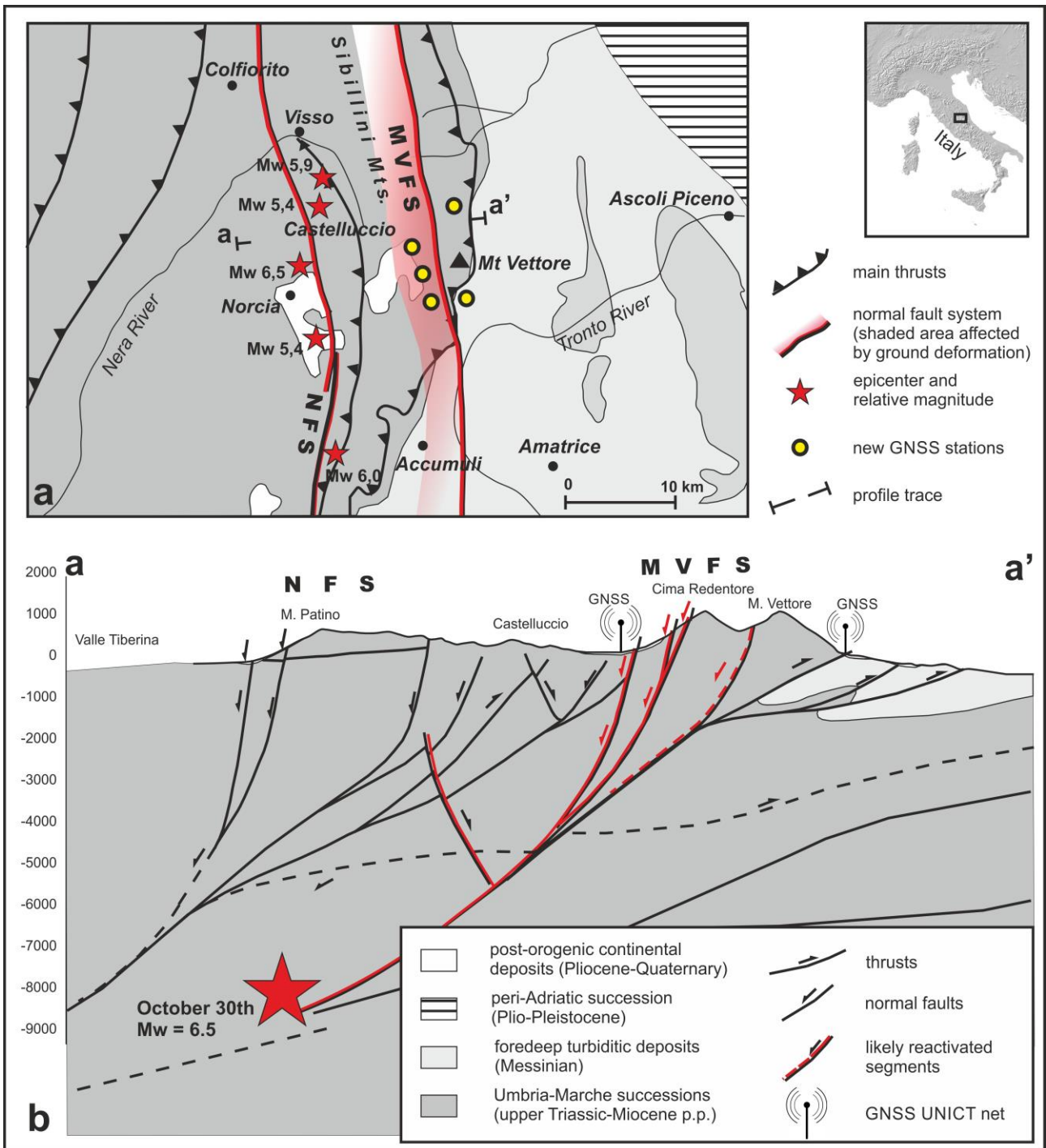
278 <http://www.isprambiente.gov.it>

279 <http://www.unavco.org/software/data-processing/teqc/teqc.html>

280 Rete Integrata Nazionale GPS - <http://ring.gm.ingv.it/>

281 [http://terremoti.ingv.it/it/ultimi-eventi/1001-evento-sismico-tra-le-province-di-rieti-e-ascoli-p-m-6-0-24-  
282 agosto.html](http://terremoti.ingv.it/it/ultimi-eventi/1001-evento-sismico-tra-le-province-di-rieti-e-ascoli-p-m-6-0-24-agosto.html); Sequenza sismica di Amatrice, Norcia, Visso: approfondimenti e report scientifici

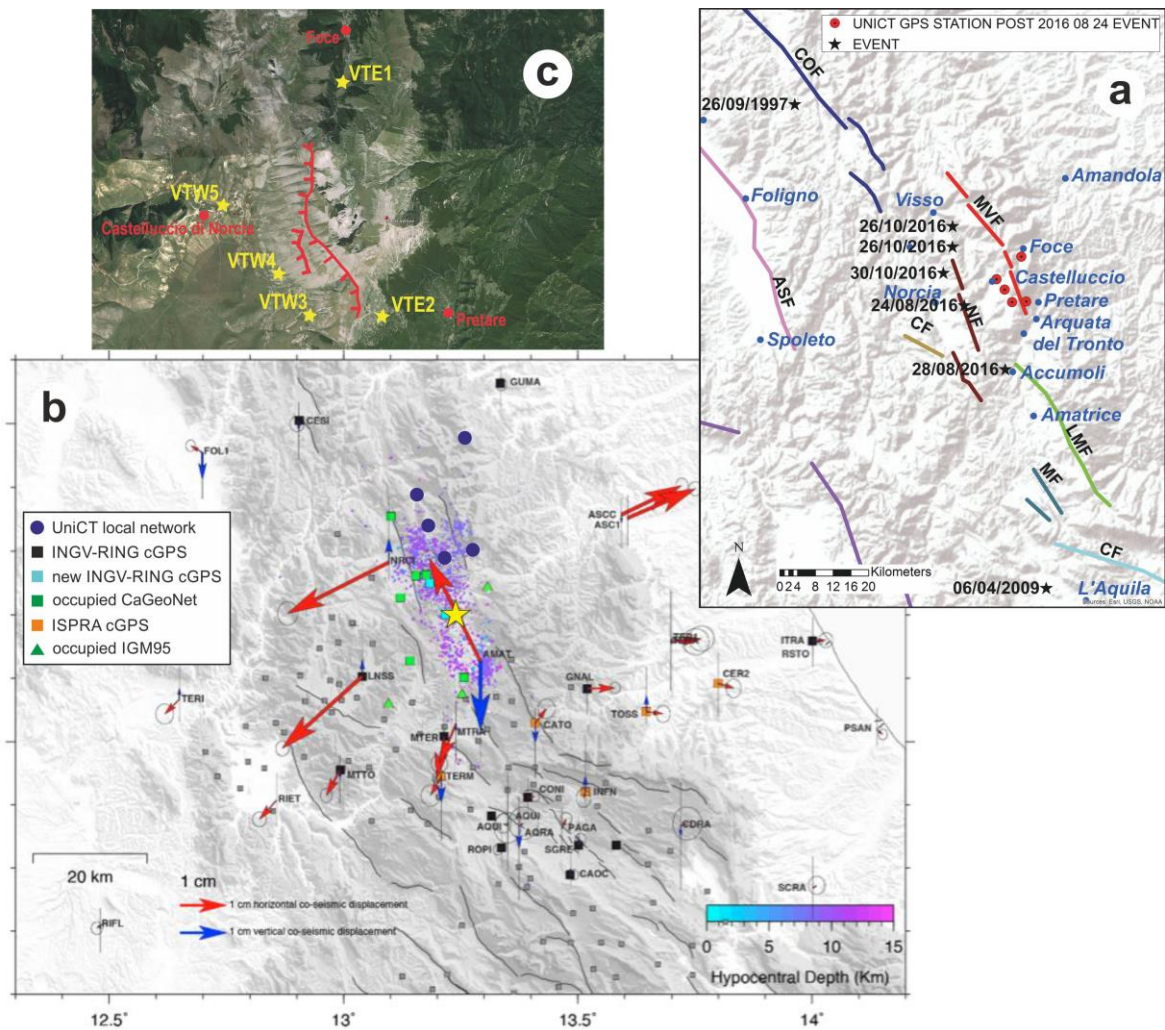
283



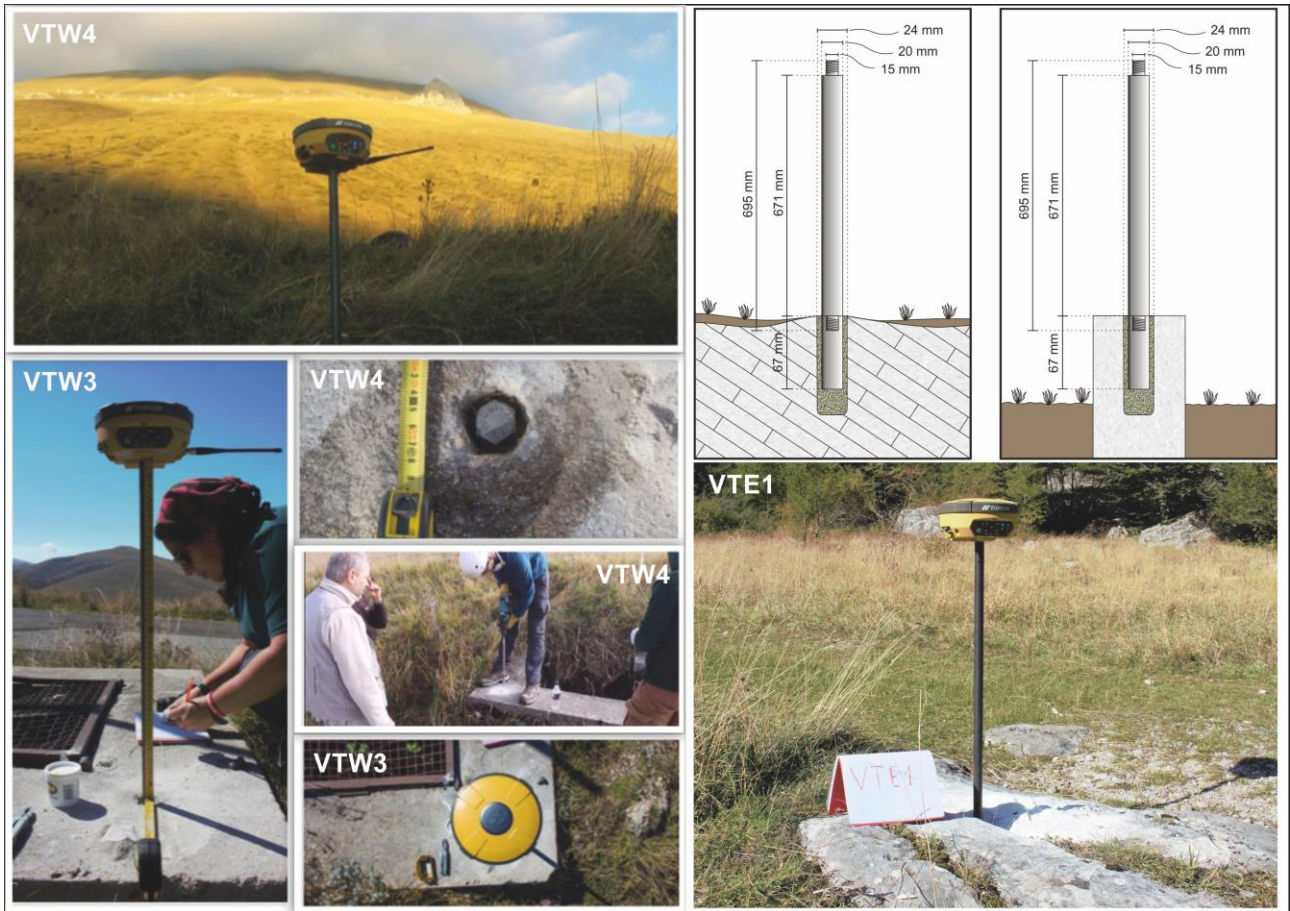
284  
285  
286  
287  
288

Fig. 1 - Simplified seismotectonic map of central Apennines (A) and geological profile across the epicentral area (B). The location of the major event (October 30<sup>th</sup>) is from GdL INGV (2016), while the main geostructural features from Pierantoni et al. (2013) and Mantovani et al. (2011) modified).



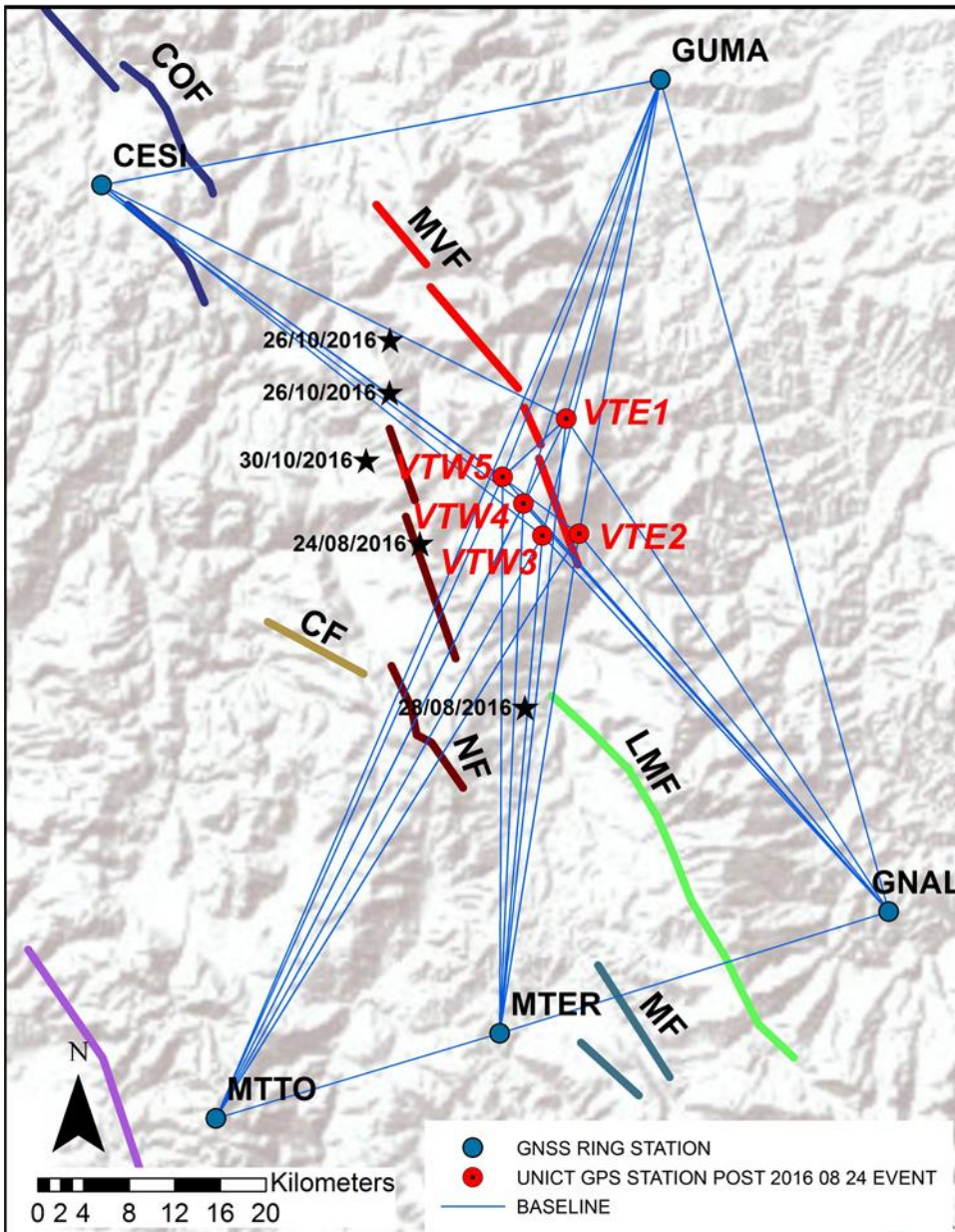


289  
 290 Fig. 2 – a) Digital Elevation Model with shaded relief of central Apennines showing the active fault system  
 291 and the major events since 1997 (ASF: Assisi Fault; COF: Colfiorito Fault; CF: Cascia Fault; MVF: Mt. Vettore  
 292 Fault; NF: Norcia Fault; LMF: Laga Mts. Fault; MF: faults of the Montereale basin). b) Horizontal (red arrows)  
 293 and vertical (blue arrows) consensus co-seismic displacements (with 68% confidence errors), and the local  
 294 UniCT GPS network. The aftershocks of the August 24<sup>th</sup>, Mw 6.0 main event (yellow star) are colored as a  
 295 function of depth (from <http://iside.rm.ingv.it>); c) GoogleEarth map showing the new five GNSS stations  
 296 (yellow stars) located in the near field (and surrounding) of the October 30th coseismic ground ruptures (red  
 297 lines).  
 298



299  
300  
301

Fig. 3 - Synoptic picture showing installation of the new GNSS stations, measurement and processing phases.



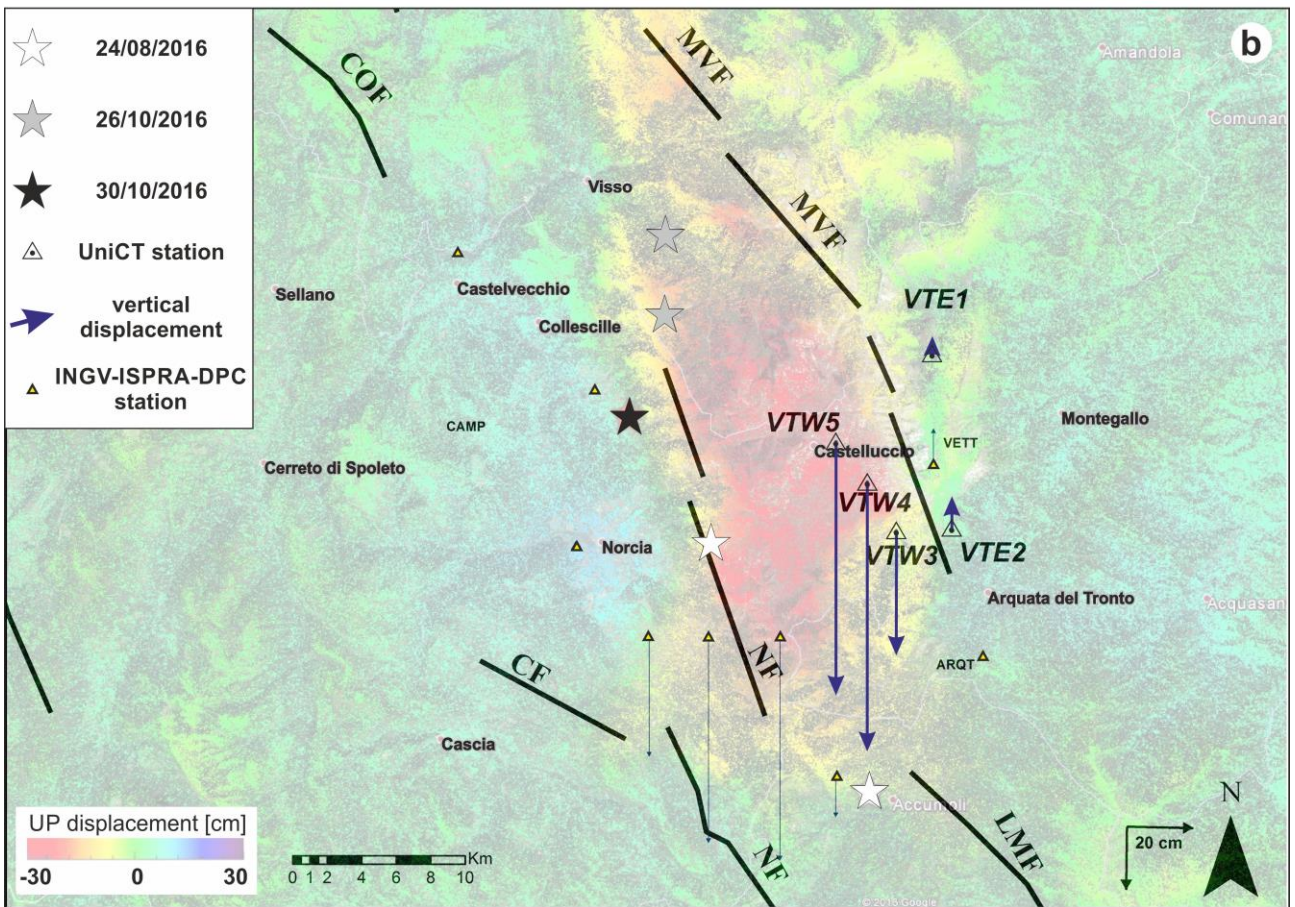
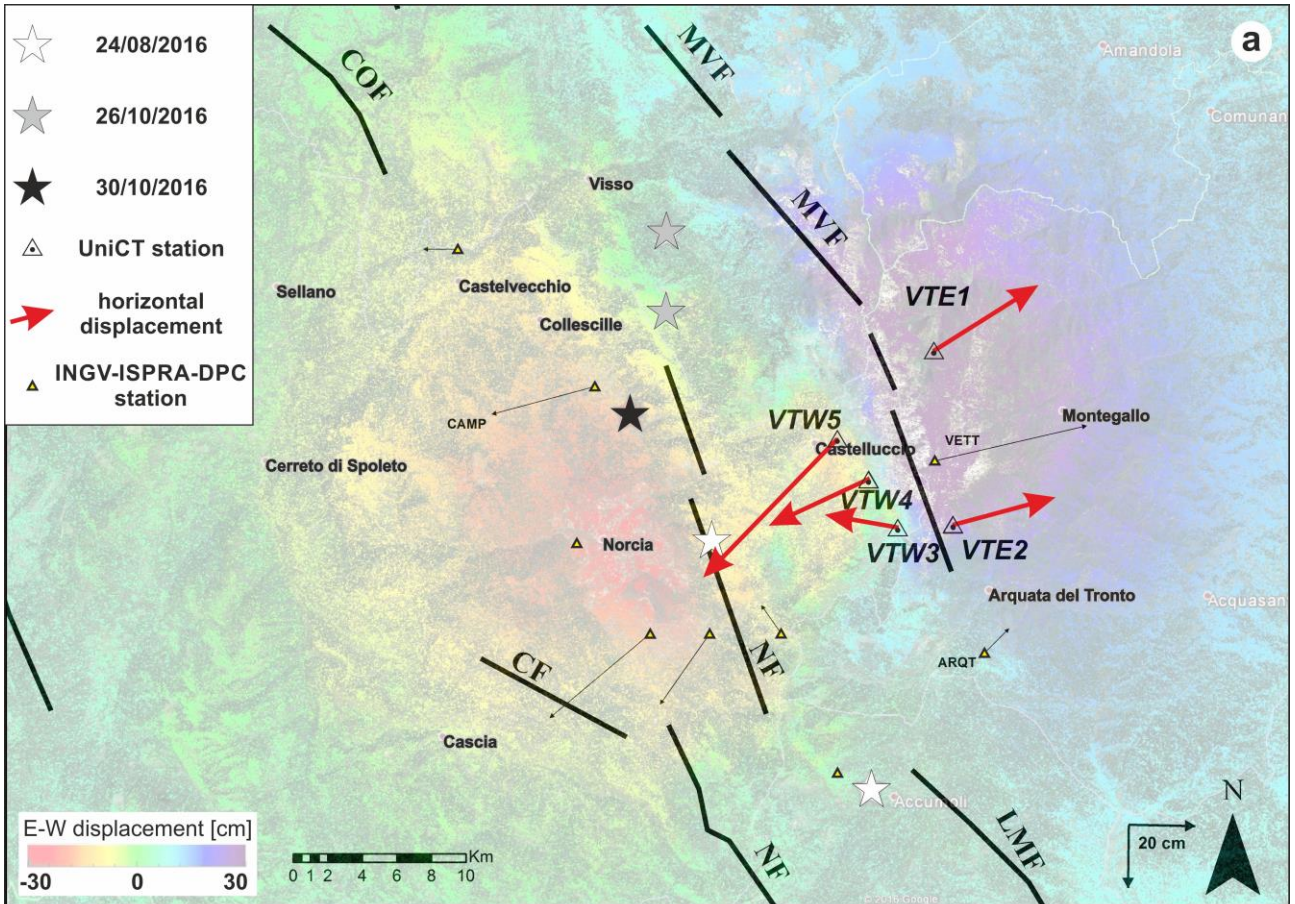
302  
303  
304  
305  
306  
307  
308  
309  
310  
311

Fig. 4 - Baselines obtained by combining the new GPS UNICT stations with selected GNSS ones from the RING Network.

312  
313  
314  
315  
316  
317

Fig. 5 - Color-coded maps showing the E-W (a) and vertical (b) displacement distribution obtained by the DInSAR technique ([http://www.irea.cnr.it/index.php?option=com\\_k2&view=item&id=761:nuovi-risultati-sul-terremoto-del-30-ottobre-2016-ottenuti-dai-radar-dei-satelliti-sentinel-1](http://www.irea.cnr.it/index.php?option=com_k2&view=item&id=761:nuovi-risultati-sul-terremoto-del-30-ottobre-2016-ottenuti-dai-radar-dei-satelliti-sentinel-1)) recorded On October 26<sup>th</sup> 2016 (pre-event images) and on November 1<sup>st</sup> 2016 (post-event images). The red and blue arrows represent the consensus pre-, co-, and post-seismic displacements (with 95% confidence errors) on the basis of the GNSS UNICT network. Epicenters of major shocks are from <http://ring.gm.ingv.it>.





319  
320

<i>ID</i>	<i>Station</i>	<i>Longitudine</i>	<i>Latitudine</i>	<i>disp<sub>N-S</sub></i>	<i>disp<sub>E-W</sub></i>	<i>disp<sub>UP</sub></i>	<i>unc<sub>N-S</sub></i>	<i>unc<sub>E-W</sub></i>	<i>unc<sub>UP</sub></i>
VTE1	FOCE_SENTIERO	13° 15' 57,45166"	42° 51' 57,04340"	141	312	29	15.5	16.5	44.0
VTE2	PRETARE	13° 16' 33,20959"	42° 47' 56,56780"	60	282	67	19.0	16.5	46.0
VTW3	QUARTUCCIOLO	13° 14' 46,41153"	42° 47' 56,57032"	198	26	-349	15.5	14.5	36.0
VTW4	COLLE_CURINA	13° 13' 55,01245"	42° 48' 59,62491"	102	288	-769	15.5	15.0	36.0
VTW5	CASTELLUCCIO_VALLE	13° 12' 56,20423"	42° 49' 54,89014"	353	418	-707	15.0	13.5	37.5

321

322

323

324

325

326

Tab 1 - Three components co-seismic displacements and relative uncertainties estimated for the GNSS stations of the UNICT network. Coordinates are WGS84 east and north, respectively. All displacement and uncertainty values are in millimeters. For all stations, the cut-off angle is 15°, the troposphere model is the Goad-Goodmar and the meteo model used is NRLMSISE. The table can be download as ASCII file on the INGVRING web page (<http://ring.gm.ingv.it>).